

VU Research Portal

Inherent characteristics of sawtooth cycles can explain different glacial periodicities

Omta, A.W.; Kooi, B.W.; van Voorn, G.A.K.; Rickaby, R.E.M; Follows, M.J.

published in

Climate Dynamics
2016

DOI (link to publisher)

[10.1007/s00382-015-2598-x](https://doi.org/10.1007/s00382-015-2598-x)

document version

Publisher's PDF, also known as Version of record

[Link to publication in VU Research Portal](#)

citation for published version (APA)

Omta, A. W., Kooi, B. W., van Voorn, G. A. K., Rickaby, R. E. M., & Follows, M. J. (2016). Inherent characteristics of sawtooth cycles can explain different glacial periodicities. *Climate Dynamics*, 46, 557-569. <https://doi.org/10.1007/s00382-015-2598-x>

General rights

Copyright and moral rights for the publications made accessible in the public portal are retained by the authors and/or other copyright owners and it is a condition of accessing publications that users recognise and abide by the legal requirements associated with these rights.

- Users may download and print one copy of any publication from the public portal for the purpose of private study or research.
- You may not further distribute the material or use it for any profit-making activity or commercial gain
- You may freely distribute the URL identifying the publication in the public portal ?

Take down policy

If you believe that this document breaches copyright please contact us providing details, and we will remove access to the work immediately and investigate your claim.

E-mail address:

vuresearchportal.ub@vu.nl

Inherent characteristics of sawtooth cycles can explain different glacial periodicities

Anne Willem Omta¹ · Bob W. Kooi² · George A. K. van Voorn³ ·
Rosalind E. M. Rickaby⁴ · Michael J. Follows¹

Received: 7 October 2014 / Accepted: 3 April 2015 / Published online: 16 April 2015
© Springer-Verlag Berlin Heidelberg 2015

Abstract At the Mid-Pleistocene Transition about 1 Ma, the dominant periodicity of the glacial-interglacial cycles shifted from ~40 to ~100 kyr. Here, we use a previously developed mathematical model to investigate the possible dynamical origin of these different periodicities. The model has two variables, one of which exhibits sawtooth oscillations, resembling the glacial-interglacial cycles, whereas the other variable exhibits spikes at the rapid transitions. When applying a sinusoidal forcing with a fixed period, there emerges a rich variety of cycles with different periodicities, each being a multiple of the forcing period. Furthermore, the dominant periodicity of the system can

change, while the forcing periodicity remains fixed, due to either random variations or different frequency components of the orbital forcing. Two key relationships stand out as predictions to be tested against observations: (1) the amplitude and the periodicity of the cycles are approximately linearly proportional to each other, a relationship that is also found in the $\delta^{18}\text{O}$ temperature proxy. (2) The magnitude of the spikes increases with increasing periodicity and amplitude of the sawtooth. This prediction could be used to identify one or more currently hidden spiking variables driving the glacial-interglacial transitions. Essentially, the quest would be for any proxy record, concurrent with a dynamical model prediction, that exhibits deglacial spikes which increase at times when the amplitude/periodicity of the glacial cycles increases. In the specific context of our calcifier-alkalinity mechanism, the records of interest would be calcifier productivity and calcite accumulation. We believe that such a falsifiable hypothesis should provide a strong motivation for the collection of further records.

Electronic supplementary material The online version of this article (doi:10.1007/s00382-015-2598-x) contains supplementary material, which is available to authorized users.

✉ Anne Willem Omta
omta@mit.edu

Bob W. Kooi
bob.kooi@vu.nl

George A. K. van Voorn
george.vanvoorn@wur.nl

Rosalind E. M. Rickaby
rosalind.rickaby@earth.ox.ac.uk

Michael J. Follows
mick@ocean.mit.edu

Keywords Sawtooth cycle · Glacial-interglacial · Mid-Pleistocene Transition · Bifurcation · Emergent phenomena

1 Introduction

Around 1 Ma, the dominant periodicity of the glacial-interglacial cycles lengthened from around 40 kyr to around 100 kyr, accompanied by an amplitude increase (Fig. 1). This so-called Mid-Pleistocene Transition (MPT) has been identified by Crucifix (2012) as a particularly attractive test case for our understanding of the glacial-interglacial dynamics. Both before and after the MPT, the orbital climate forcings with the highest amplitude have been precession, with

¹ EAPS Department, Massachusetts Institute of Technology, 77 Massachusetts Avenue, Cambridge, MA 02139, USA

² Faculty of Earth and Life Sciences, VU University, De Boelelaan 1081, 1081 HV Amsterdam, The Netherlands

³ Biometris, Wageningen University and Research Centre, PO Box 16, 6700 AA Wageningen, The Netherlands

⁴ Department of Earth Sciences, Oxford University, Parks Road, Oxford OX1 3PR, UK

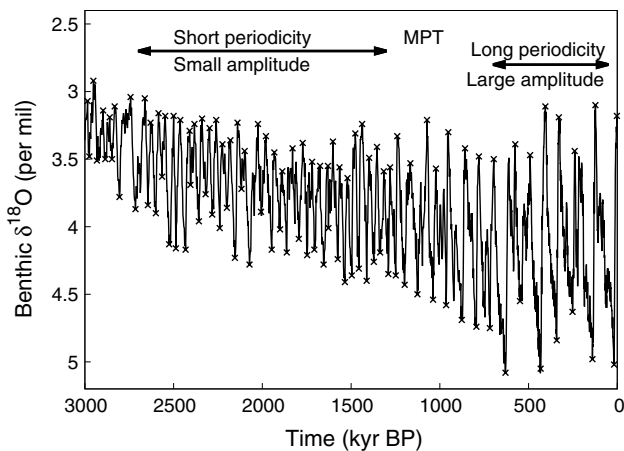


Fig. 1 Marine $\delta^{18}\text{O}$, a proxy for global ice volume and ocean temperature, over the past 3 Myr (Lisiecki and Raymo 2005). The MPT is clearly visible as a shift in the periodicity and amplitude of the glacial-interglacial cycles. Note that time goes forward to the right. The crosses indicate glacial and interglacial minima and maxima used in the determination of the lengths and amplitudes of the cycles for Fig. 8b

a periodicity of ~ 20 kyr, and obliquity, with a periodicity of ~ 40 kyr; the ~ 100 -kyr eccentricity component has always been much weaker (Imbrie et al. 1993). Although the amplitudes of these forcings have been varying continuously, they did not consistently increase or decrease through the MPT (Berger and Loutre 1991).

Most hypotheses to explain the MPT have focused on internal changes in the responding Earth system. It has been speculated that a gradual CO_2 decrease throughout the Pleistocene culminated in the carbon cycle becoming unstable, leading to the large-amplitude, long-periodicity sawtooth cycles of the Late Pleistocene (Saltzman and Maasch 1991), but the specific mechanism behind such an instability is unclear. Various models have assumed that deglaciations are triggered by insolation, after the ice volume or temperature has crossed a threshold value (Paillard and Parrenin 2004; Huybers and Wunsch 2005). The general cooling due to a CO_2 decrease during the Pleistocene could have demanded a greater increase in the insolation to trigger a glacial-interglacial transition (Paillard 1998; Berger et al. 1999). Therefore, the transitions would have started to occur only every 100 kyr. However, some of the glacial-interglacial transitions after the MPT occurred when insolation was relatively low (particularly Termination 5) and there does not appear to be a clear relationship between the timing of the deglaciations and the rate of change of insolation either (Denton et al. 2010). According to a hypothesis brought forward by Tziperman and Gildor (2003), the cooling climate would have pushed the system from a regime with

a linear response to orbital forcing to a nonlinear regime with sawtooth cycles in land ice and spikes in sea ice (Gildor and Tziperman 2001). Crowley and Hyde (2008) proposed that the MPT is a step towards a new stable climate state characterized by permanent mid-latitude Northern Hemisphere glaciation.

A different line of thought focuses on the internal dynamics of the Laurentide ice sheet covering North America during glacial times (Clark and Pollard 1998). This ice sheet was first grounded, for the most part, on soft sediments, but gradual soil erosion allowed more of the ice sheet to be in direct contact with hard bedrock. It was hypothesized that this solid foundation then allowed the ice sheet to grow thicker and oscillate more slowly in the Late Pleistocene. Alternatively, the MPT could simply reflect the increasing importance of the Laurentide ice sheet. According to Raymo et al. (2006), there was a dominant 41-kyr periodicity in marine $\delta^{18}\text{O}$ records before the MPT, because precession-driven variations in ice volume in the Northern and Southern Hemispheres cancelled each other. At the MPT, the Northern Hemisphere ice-sheet fluctuations would have become the primary control on Antarctic ice volume. Bintanja and van de Wal (2008) argued that the Fennoscandian ice sheet in Northern Europe initially contributed most to the total Northern Hemisphere ice volume, with the Laurentide ice sheet taking over at the MPT. Ditlevsen (2009) stated that approximately between 800 ka and 1 Ma, the ‘deep glacial state’ hypothesized by Paillard (1998) became accessible resulting in a change in the length of the cycles. This seems consistent with an increase in the ice volume at peak glacial times around 900 kyr (Mudelsee and Schulz 1997; Elderfield et al. 2012), but it remains unclear whether this increase in peak ice volume is the cause or the consequence of the MPT.

Some hypotheses to explain the MPT have focused on the orbital forcing. For example, Schulz and Zeebe (2006) pointed out that close to each of the last 7 glacial-interglacial transitions, there was a relatively long period of time when insolation increased in both Northern and Southern hemispheres. This may have helped produce transitions with a large amplitude. Rial et al. (2013) suggested that the 100-kyr cycles emerged, because the climate system became frequency-modulated by the 413-kyr component of the eccentricity of the Earth’s orbit. This frequency modulation could lead to a power transfer from the 413-kyr to the 100-kyr band. Indeed, Rial et al. (2013) showed that over the past 2 Myr, the spectral power of the glacial cycles increases in the 100-kyr band, with a simultaneous power decrease in the 413-kyr band. However, it needs to be noted that the power increase in the 100-kyr band is orders of magnitude larger than the power decrease in the

Table 1 Description of variables (var) and parameters (par) of the calcifier-alkalinity model, including respective units and meaning, along with parameter values

Var	Units	Meaning	
t	yr	Time	
A	mol eq m^{-3}	Alkalinity	
C	mol m^{-3}	Calcifier population size	
Par	Units	Meaning	Value
I	$\text{mol eq m}^{-3} \text{ yr}^{-1}$	Alkalinity input	4×10^{-6}
k	$(\text{mol eq})^{-1} \text{ m}^3 \text{ yr}^{-1}$	Reaction rate	0.05
M	yr^{-1}	Mortality rate	0.1
α	–	Periodic forcing amp.	Variable
ε	–	Random forcing amp.	0.005

413-kyr band. Furthermore, Rial et al. (2013) provided no explanation why a 413-kyr frequency modulation should lead to a strong 100-kyr periodicity beyond that it must be due to a nonlinear mechanism. Nevertheless, the complexity of the Earth system is such that the Rial et al. (2013) mechanism cannot be excluded. In fact, this is only one example of the complex behavior of periodically forced systems. Very simple forced systems, such as elementary ice-sheet and ecological models or even a pendulum, exhibit various bifurcations, phase locking, and chaos (le Treut and Ghil 1983; Miles 1988; Kuznetsov et al. 1992; Rinaldi and Muratori 1993; Ghil 1994; Mitsui and Aihara 2014).

Huybers (2009) proposed that switches in the dominant periodicity of the climate system may occur spontaneously, without a change in the system parameters. A key assumption behind the Huybers (2009) model is that the climate system possesses a memory: after a cold glacial period, the ice sheets should melt at a faster rate than after a relatively mild glacial. Although tantalizing, the memory hypothesis is not specific enough to be tested against observations. In this paper, we demonstrate that it is not necessary to impose an explicit memory on the system to obtain changes in the dominant periodicity without a change in the system parameters. Rather, we argue that such changes are an inherent feature of sawtooth-spike oscillations, which the glacial-interglacial cycles resemble. We use the previously developed calcifier-alkalinity model (Omta et al. 2013) as an illustrative example of a system exhibiting sawtooth-spike behavior. Within the context of this model, the rapid deglaciations and the different glacial periodicities need to be related to atmospheric CO_2 . However, the key relationships may also apply to models based on ice dynamics, since the different periodicities appear inherent to externally forced sawtooth-spike

cycles. In fact, Crucifix (2013) has demonstrated that various models for glacial-interglacial cycles can exhibit different periodicities when forced with the Berger (1978) insolation curve (although in very limited parameter ranges in some cases). The periodically forced calcifier-alkalinity system (briefly described in Sect. 2) displays cycles with short and long periodicities, akin to the glacial cycles before and after the MPT (Sect. 3), that are investigated through a combination of numerical techniques (described in detail in Appendix 1). To investigate whether these periodicities still emerge in a more realistic setup that includes vertical and horizontal structure, we have also performed two simulations with a more elaborate multi-box model (Appendix 2); similar relationships are found as with the simplest formulation. In Sect. 4, we discuss the dynamical origin of the different periodicities and their potential relation to the MPT. We finish with our main conclusions, along with a suggestion how they may be falsified (Sect. 5).

2 Model

We use the calcifier-alkalinity model that has been described and discussed in detail in Omta et al. (2013); the model code, including brief instructions, has been attached as online Auxiliary Material. In its simplest version, the model consists of two differential equations for ocean alkalinity A and a calcifier population C (variables and parameter values listed in Table 1):

$$\frac{dA}{dt} = I - kAC \quad (1a)$$

$$\frac{dC}{dt} = kAC - MC \quad (1b)$$

Alkalinity A is added to the ocean at a fixed rate I through river runoff resulting from weathering and consumed by a population of calcifiers C , growing at an effective rate kA and sedimenting at a rate M . The autocatalytic process described in the set of Eq. (1) is sufficient to generate sawtooth-shaped oscillations in alkalinity. Alkalinity increases slowly due to a net weathering input, until a spike in the number of calcifiers leads to a rapid alkalinity drop.¹ After the spike, there is again a net alkalinity input and the cycle starts anew. For the processes considered in the model (silicate/calcite weathering, calcite production/sedimentation), alkalinity input is associated with uptake of CO_2 from the atmosphere, while alkalinity output is associated with release of CO_2 from the ocean to the atmosphere. Thus, the modeled sawtooth cycles in alkalinity correspond to CO_2 variations with the characteristic reverse sawtooth shape observed in ice-core records (Augustin et al. 2004; Lüthi et al. 2008).

The eigenvalues of the Jacobian matrix of the model system are orders of magnitude different which can lead to numerical instability when using forward integration methods. We use the MATLAB solver ode15s specifically designed for such ‘stiff’ problems. To further improve numerical stability, we introduce the transformation $P \equiv \ln C$, so that the Eq. (1) become:

$$\frac{dA}{dt} = I - kAe^P \quad (2a)$$

$$\frac{dP}{dt} = kA - M \quad (2b)$$

Various regions of the ocean floor exhibit orbitally paced variations in calcite content throughout the past 100 Myr (Herbert 1997). As in Omta et al. (2013), we therefore apply a periodic forcing to the reaction rate parameter k which directly impacts the calcifier population growth rate:

$$k = k_0 \left(1 + \alpha \cos \left(\frac{2\pi t}{T} + \theta \right) \right) \quad (3)$$

with $k_0 = 0.05 \text{ yr}^{-1} (\text{mol eq/m}^3)^{-1}$, forcing amplitude α and phase angle θ . If not explicitly stated, we take $\theta = 0$. Although there exist orbital forcings with various periodicities that could influence the dynamics, we start with

a single forcing period to facilitate a transparent analysis. In all simulations except one, we use a period $T = 20 \text{ kyr}$, because observations from the Equatorial Indian Ocean (Beaufort et al. 1997) have indicated particularly strong precessional cycles in coccolithophore productivity over the past 900 kyr. In Beaufort et al. (1997), it is argued that this could be due to insolation-forced variations in upwelling patterns. Alternatively, the calcifier productivity could be directly impacted by temperature or by the light intensity.

The climate system exhibits much variation on time-scales ranging from the weather to multiple millennia which together have the character of red noise (Peltier 1998; Huybers and Curry 2006). If the calcifiers are impacted by orbital cycles, then it seems likely that they are also impacted by these higher-frequency variations. To investigate the potential impact of such variations, we add a random component to the forcing in some of the simulations:

$$k = k_0 \left(1 + \alpha \cos \left(\frac{2\pi t}{T} \right) + \varepsilon \right) \quad (4)$$

with ε a small random number that is drawn every 1 kyr from a normal distribution with mean 0. Although the observed climatic variations have a red-noise character, we implement a simple white-noise forcing, again because we believe that keeping the model as simple as possible facilitates a transparent analysis. The simulations including white-noise forcing are performed with an Euler-forward scheme using a constant small time step of 0.01 yr.

The actual insolation is a complex quasi-periodic function that is different for each latitude and each season. To investigate the sensitivity of the system to such a complex forcing, we apply the 35-component astronomical forcing used by Saedeleer et al. (2013):

$$k = k_0 \left(1 + \alpha \sum_{i=1}^{35} \frac{s_i \sin(\omega_i t) + c_i \cos(\omega_i t)}{\sqrt{s_{16}^2 + c_{16}^2}} \right) \quad (5)$$

with coefficients s_i , c_i , ω_i taken from Saedeleer et al. (2013); we have scaled the forcing by the amplitude of the strongest component (number 16) to enable a comparison with the results obtained under the periodic forcing.

3 Results

We investigate the different behaviors of our forced system and their potential relationships with the MPT. We first analyze the emergence of periodicities different from the forcing, followed by a focus on periodicity shifts. We use concepts specific to the theory of dynamical systems (such as limit

¹ The change in ocean alkalinity corresponding with the change in atmospheric CO_2 at a typical glacial-interglacial transition is around 0.1–0.2 mol eq/m³. To estimate an upper boundary on the needed alkalinity output, consider a very rapid glacial transition, occurring in 2000 years. Even then, the net alkalinity output rate would be about 10¹⁴ mol eq/yr. This number does not seem too extreme, as Milliman et al. (1999) have estimated the current total calcite accumulation at the ocean floor to be about 2×10^{13} mol eq/yr.

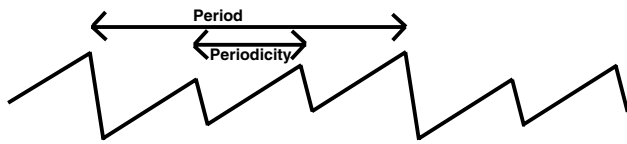


Fig. 2 A schematic depiction of what we mean by ‘period’ and ‘periodicity’: the average time from one global or local maximum to the next global or local maximum is a ‘periodicity’, whereas a ‘period’ is the time from one global maximum to the next global maximum

cycle, attractor, bifurcation) that are explained in various textbooks (Guckenheimer and Holmes 1985; Wiggins 1990).²

In Omta et al. (2013), simulations were performed with the most idealized version of the calcifier-alkalinity model under a 20-kyr sinusoidal forcing with relative amplitude $\alpha = 0.0025$ (that is, variations in the parameter k were a factor 0.0025, or 0.25 % around the mean). The system exhibited cycles with the same periodicity as the forcing. As we now increase the forcing amplitude α , there emerge different new cycles with periodicities that are multiples of the forcing period. The stronger forcing tends to ‘kick’ the system further from equilibrium which means that the cycles can obtain a larger amplitude and, due to the sawtooth shape, a correspondingly longer periodicity. For forcing amplitude $\alpha = 0.004$, cycles with periodicities of 20, 40, 60, 80, 100 kyr coexist (in Fig. 3, 40- and 100-kyr cycles are shown to contrast long and short periodicities); which periodicity the system lands upon depends subtly on the initial conditions.

To gain a deeper understanding of how the different cycles relate to each other, we perform a bifurcation analysis with the numerical package AUTO (see Appendix 1 for a technical explanation). We use the forcing amplitude α as a bifurcation parameter; the results are presented in the form of a bifurcation diagram (Fig. 4). The attractor branch originating at the vertical axis corresponds with a limit cycle with a 20-kyr period and an approximately sinusoidal shape. At forcing amplitude $\alpha \approx 0.004$, this branch bends backward at a tangent bifurcation point, becoming a saddle limit cycle. When the saddle branch has almost reached the

² In some cases, applied mathematicians and earth scientists use similar words with somewhat different meanings which can cause confusion. To be precise in our terminology, we make a distinction between ‘period’ and ‘periodicity’ that is schematically clarified in Fig. 2. According to the mathematical definition, a periodic signal repeats itself exactly. The maximum value reached during one period is exactly the same as the maximum value during the next period. Thus, a periodic signal has an infinite number of global maxima. With ‘period’ we mean the time from one global maximum to the next (top arrow in Fig. 2). Between two global maxima, a periodic signal may also exhibit lower maxima. With ‘periodicity’ we mean the average time from one local maximum to the next (lower arrow in Fig. 2). For regular periodic functions, such as sinusoids, the period and periodicity are the same and the two terms can be used interchangeably.

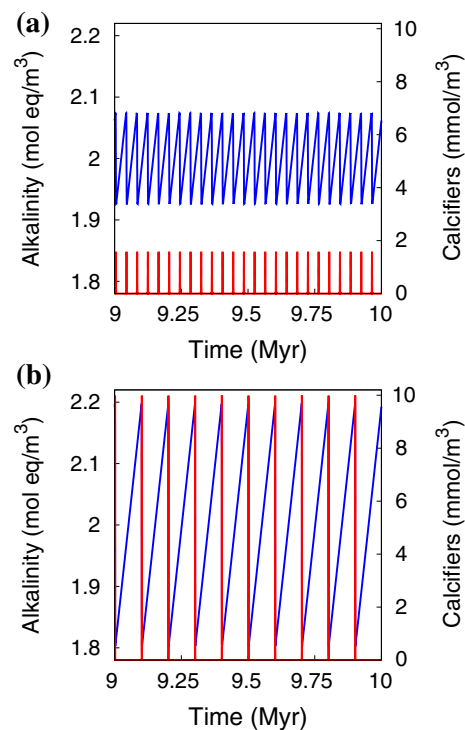


Fig. 3 Under a periodic forcing with the same period (20 kyr) and amplitude ($\alpha = 0.004$), the calcifier-alkalinity model can give rise to oscillations with very different periodicities. The last 1 Myr of two 10-Myr simulations with different initial conditions (alkalinity blue and calcifiers red): **a** $A_0 = 2.0 \text{ mol eq/m}^3$, $C_0 = 2.0 \times 10^{-3} \text{ mol/m}^3$, leading to an oscillation with a 40-kyr periodicity; **b** $A_0 = 2.0 \text{ mol eq/m}^3$, $C_0 = 0.01 \text{ mmol/m}^3$, leading to an oscillation with a 100-kyr periodicity

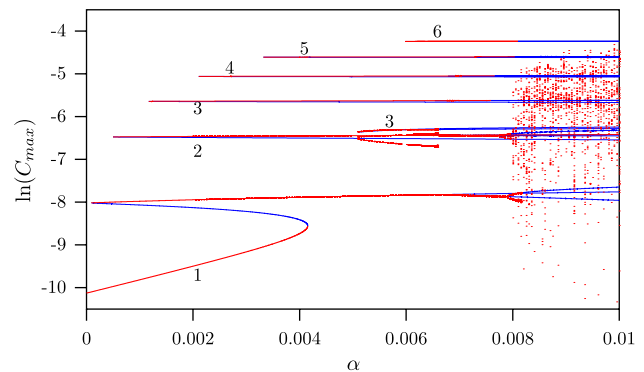


Fig. 4 Bifurcation diagram with the forcing amplitude α on the horizontal axis and $\ln(C_{max})$ on the vertical axis, with C_{max} (mol/m³) the global maximum calcifier concentration reached. Red branches are stable limit cycles, blue branches are unstable limit cycles. The numbers next to the branches refer to the periodicities of the limit cycles in terms of integers multiples of the forcing period, that is, 1 means $1 \cdot 20 = 20$ kyr, 2 means $2 \cdot 20 = 40$ kyr, etc

vertical axis, it bends forward at a second tangent bifurcation point and becomes again an attractor limit cycle. This limit cycle still has a 20-kyr period, but its amplitude is

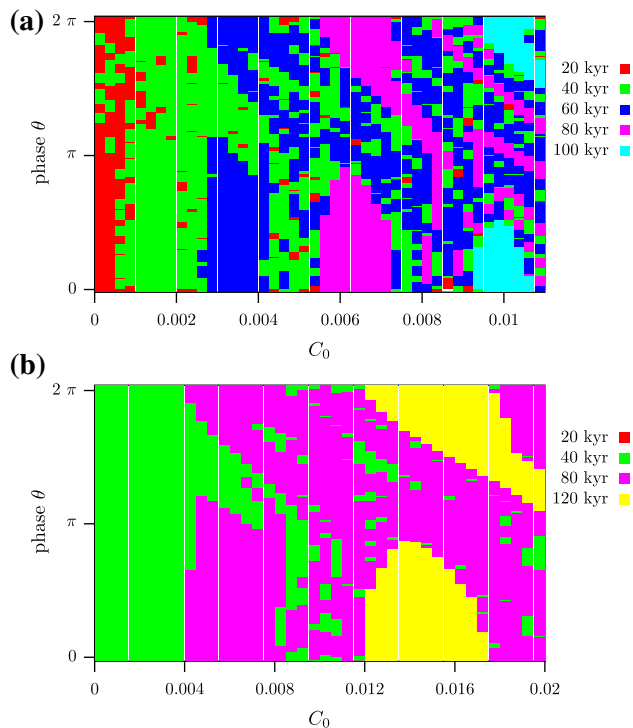


Fig. 5 Periodicity of the asymptotic limit cycle as a function of the initial calcifier concentration and phase of the forcing, with the initial alkalinity kept at 2.0 mol eq/m^3 , for **a** forcing period $T = 20 \text{ kyr}$ and $\alpha = 0.004$: red 20 kyr, green 40 kyr, dark blue 60 kyr, purple 80 kyr, light blue 100 kyr; **b** forcing period $T = 40 \text{ kyr}$ and $\alpha = 0.008$: green 40 kyr, purple 80 kyr, yellow 120 kyr. At the lower horizontal axis, the initial calcifier concentration C_0 is depicted, with the initial phase of the forcing θ on the vertical axis. Note the intricately curved basins of attraction

much larger, with the alkalinity variations having more of a sawtooth shape. Depending on the initial state, the system can land in either the small-amplitude 20-kyr cycle or the larger-amplitude 20-kyr cycle. Following the 20-kyr branch further in the system, it goes through an infinite number of period doublings, before it becomes chaotic at $\alpha \approx 0.008$. In the chaotic regime, there are scattered points that indicate local maxima instead of recognizable branches, because the maximum calcifier concentration varies all the time. The various cycles with periodicities that are multiples of the forcing period (Fig. 3) are represented by the unconnected upper branches in the bifurcation diagram (Fig. 4). These cycles do not emerge from period-doubling bifurcations, but are rather due to nonlinear resonance. For a large range of forcing amplitudes (i.e., $0.0035 < \alpha < 0.007$), stable branches of the 20-, 40-, 60-, 80-, and 100-kyr cycles all exist, and a 120-kyr branch emerges at $\alpha \approx 0.006$. This suggests that a shift from one periodicity to another could occur because of a temporary disturbance or some noise without a parameter change.

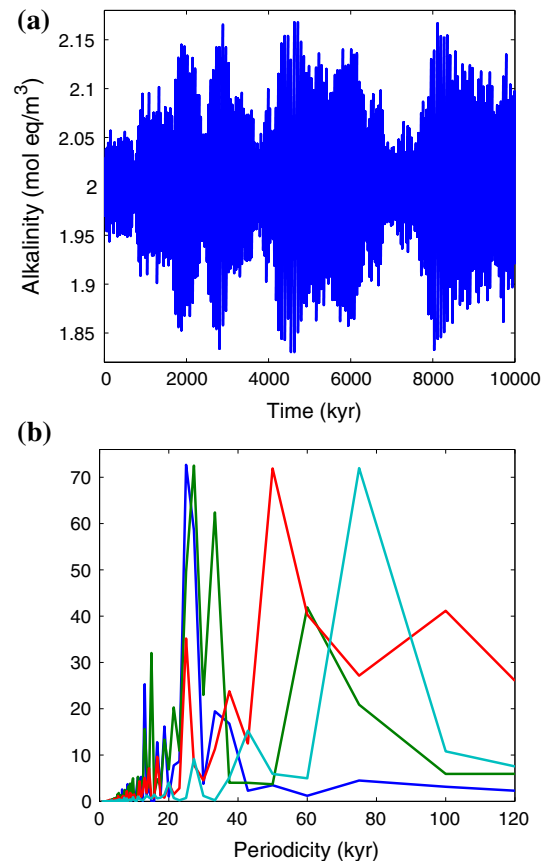


Fig. 6 Shifts in the dominant periodicity can occur due to a random component in the forcing. Simulation results for $\alpha = 0.004$ with noise forcing ε with standard deviation 0.005, with initial conditions $A_0 = 2.0 \text{ mol eq/m}^3$, $C_0 = 1.0 \times 10^{-4} \text{ mol/m}^3$: alkalinity as a function of time **(a)** and Fourier periodogram **(b)** of A for 0–300 kyr (blue), 7.4–7.7 Myr (green), 8.0–8.3 Myr (light blue), 9.7–10 Myr (red); the spectra have been rescaled for easy comparison

To investigate the likelihood of such periodicity shifts, we determine the basins of attraction of the different limit cycles. We perform a large set of 80-Myr simulations in which the initial calcifier concentration C_0 and the initial phase of the forcing θ are varied, while the initial alkalinity A_0 is kept fixed at 2.0 mol eq/m^3 (Fig. 5a). The basins of attraction are intricately curved which means that the asymptotic behavior is highly sensitive to the initial conditions. Moreover, the patchwork of periodicities makes periodicity shifts driven by disturbances likely. A key observation is that adjacent basins of attraction correspond to limit cycles with widely different periodicities. For example, there exist 60-kyr (dark blue) limit cycles right next to the 100-kyr (light blue) regions in Fig. 5a. Minor noise can already result in the system switching between these limit cycles, without the need to step through 20-kyr periodicity increments. To investigate the potential role of obliquity,

we increase the forcing period to 40 kyr (Fig. 5b). There are robust 40-, 80-, and 120-kyr periodicities, but no robust 100-kyr period or periodicity, simply because 100 is not a multiple of 40. Hence, it appears unlikely that the 100-kyr cycles after the MPT are primarily driven by the obliquity variations.

Clearly, the system possesses a rich variety of limit cycles between which it could switch. In general, it transiently goes between different dominant periodicities before it lands upon its asymptotic limit cycle. If a random component is added to the forcing, the system can keep switching between periodicities. In the 10-Myr simulation shown in Fig. 6, no steady limit cycle is reached. Furthermore, the dominant periodicity is often a multiple of 20 kyr, but not always, even after many Myr of simulation.³ In the Earth system, there is a red-noise background (due to the weather and climatic variations on scales from years to multiple millennia) which is why truly stable cycles probably do not exist. The system may spend a considerable amount of time in one domain of attraction, but random variations will inevitably shoot it to a different state at some point. Further simulations using the quasi-periodic forcing of Saedeleer et al. (2013) indicate that the presence of multiple frequency components in the orbital forcing can have an impact similar to noise (which has an infinite number of frequency components), helping the system switch between various periodicities (Fig. 7).

Throughout our simulations, the limit cycles with various periodicities possess two key features that stand out as testable predictions:

1. The periodicity and the amplitude of the cycles are approximately linearly proportional to each other. This is essentially due to the sawtooth geometry: a longer duration of the slow linear increase implies a proportionately larger amplitude of the cycle and vice versa. To test this relationship against the observations, we have first visually identified the glacial minima and interglacial optima of the last 3 Myr from the Lisiecki and Raymo (2005) record (crosses in Fig. 1). Subsequently, we have determined the amplitude of each

³ Random variations or noise in relation to the MPT have been considered earlier by Saltzman and Maasch (1991) and Ditlevsen (2009), but both studies are fundamentally different from our work. Ditlevsen (2009) inferred a bifurcation structure that would lead to periodicity shifts and from there constructed a model with this bifurcation structure. Our model was constructed to describe the sawtooth shape of the glacial cycles. It exhibits periodicity shifts as an emergent property, rather than as an imposed feature. Saltzman and Maasch (1991) suggested that the Earth System went through a bifurcation at the MPT due to the decreasing average atmospheric $p\text{CO}_2$. Our simulations indicate, similar to Huybers (2009), that a sawtooth system can exhibit a periodicity shift without going through a bifurcation.

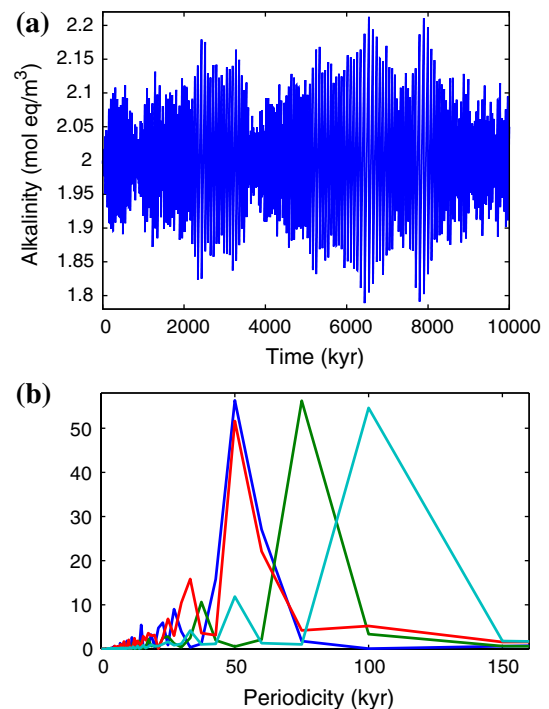


Fig. 7 Shifts in the dominant periodicity can also occur due to the presence of various frequency components in the orbital forcing. Simulation results with the quasi-periodic forcing described by Eq. (5) for $\alpha = 0.0046$, with initial conditions $A_0 = 2.0 \text{ mol eq/m}^3$, $C_0 = 1.0 \times 10^{-4} \text{ mol/m}^3$: alkalinity as a function of time (a) and Fourier periodogram (b) of A for 300–600 kyr (blue), 3.0–3.3 Myr (green), 6.4–6.7 Myr (light blue), 9.7–10 Myr (red); the spectra have been rescaled for easy comparison

cycle as the difference in terms of ‰ $\delta^{18}\text{O}$ between the glacial minimum and the preceding interglacial optimum, and the length or periodicity as the amount of time between subsequent interglacial optima. In Fig. 8, we show the amplitudes plotted against the periodicities of the cycles according to the model and according to the $\delta^{18}\text{O}$ record: both exhibit approximately linear relationships, with slopes corresponding with the slow part of the sawtooth.

2. The magnitude of the calcite accumulation spikes increases with increasing periodicity and amplitude of the sawtooth. To test this relationship, we have searched for records of calcite accumulation, C_{37} alkenones, and total organic carbon⁴ spanning across periods of time when the amplitude of the glacial cycles

⁴ Calcite accumulation records reflect both calcite production and preservation, whereas C_{37} alkenones are a proxy for coccolithophore productivity specifically (Marlowe et al. 1990). Total organic carbon is a proxy for total export production, although it is also impacted by variations in preservation and dilution with other sediment components (Schoepfer et al. 2015).

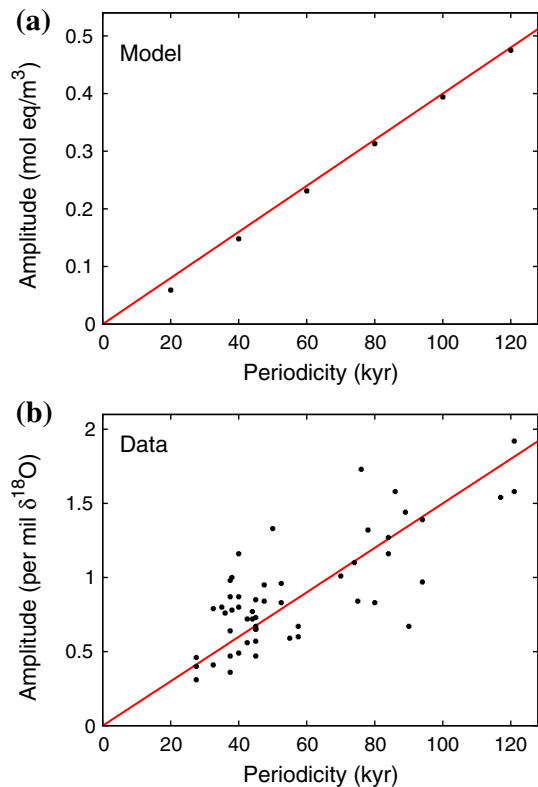


Fig. 8 The periodicity and the amplitude of the cycles are approximately linearly proportional to each other, both in the calcifier-alkalinity model (a) and in the data (b). To create (a), we have performed 6 simulations with $\alpha = 0.0063$ and initial conditions $A_0 = 2.0$ mol eq/m³ (all), $C_0 = 0.0003$ mol/m³ (20 kyr), $C_0 = 0.001$ mol/m³ (40 kyr), $C_0 = 0.004$ mol/m³ (60 kyr), $C_0 = 0.010$ mol/m³ (80 kyr), $C_0 = 0.016$ mol/m³ (100 kyr), $C_0 = 0.014$ mol/m³ (120 kyr) and determined the amplitudes corresponding with the various periodicities. To create (b), we have determined the length and the amplitude of each individual glacial cycle over the past 3 Myr in the Lisiecki and Raymo (2005) data set. The crosses in Fig. 1 indicate glacial and interglacial minima and maxima used in the determination of the lengths and amplitudes of the cycles. The red line in (a) corresponds with the constant weathering input of alkalinity $I = 0.004$ mol eq m⁻³/kyr. The red line in (b) is a linear fit to the data ($r^2 = 0.6$); the fitted slope of 0.015 ‰ $\delta^{18}\text{O}$ /kyr (or 1.5 ‰ per 100 kyr) is similar to the typical rate of decline going from an interglacial into a glacial period

increased (Early Pleistocene, MPT, Mid-Brunhes Event). Some records do not show clear deglacial spikes (Liu and Herbert 2004; Sexton and Barker 2012), but the records that exhibit spikes also tend to show an increase in the magnitude of the spikes when the amplitude of the glacial-interglacial cycles increases. This is observed for total organic carbon at ODP Site 1143 (South China Sea) across the Early Pleistocene (Tian et al. 2006), C_{37} alkenones at ODP Site 1077 (Angola Basin) across the MPT (Schefuss et al. 2005), and calcite accumulation at ODP Site 1094 (Southern Ocean) across the Mid-Brunhes

(Jaccard et al. 2013). Hence, there is observational support for this prediction, although many more records of calcite accumulation and calcifier productivity will need to be collected for a thorough test.

Both in Omta et al. (2013) and in the current study (Appendix 2), we included simulations with a multi-box model for comparison. We found it reassuring that the more explicit model gave similar predictions as our simple formulation. However, we had to make many more assumptions about parameter values for the multi-box model, while the added complexity did not lead to further testable predictions beyond the ones provided by the simple model. This provided further motivation to focus our extensive analysis on the most idealized formulation.

4 Discussion

Our forced system exhibits limit cycles with periodicities that are integer multiples of the forcing period, as well as periodicity shifts triggered by either random variations or different frequency components of the orbital forcing. The various periodicities originate in the interaction between the forcing, the sawtooth alkalinity and the spiking calcifiers. The calcifiers do better at forcing maxima, but this is not a sufficient condition for a spike: the alkalinity needs to be high enough for the calcifiers to increase. If the alkalinity is low, then the calcifiers will ‘wait’ for another forcing maximum. Even after the alkalinity has increased above the mean value, the calcifiers can be at a too low level to spike quickly, so they may ‘skip’ yet more forcing cycles before finally spiking and inducing a rapid drop in the alkalinity.

Although threshold models can generate glacial cycles with a different periodicity than the forcing (Paillard 1998; Huybers 2007), the periodicity and amplitude of the glacial cycles remain approximately the same, unless the threshold or another system parameter changes. Huybers (2009) demonstrated that spontaneous changes in the periodicity are possible, if the system remembers the preceding glacial during the glacial-interglacial transition. In the model system presented here, the calcifiers provide a possible mechanistic underpinning to the memory hypothesized by Huybers (2009), because they tend to spike to a higher level at the end of a large glacial period with a particularly high alkalinity. In our view, this finding provides evidence for the presence of a spiking variable in the climate system that plays an active role in glacial dynamics. Moreover, we think that the presence of a key spiking variable is likely, simply because the derivative of a sawtooth oscillation is a series of spikes. This is also why many models for glacial-interglacial cycles exhibit sawtooth-spike behavior. In the sea-ice switch model (Gildor and Tziperman 2000, 2001; Tziperman et al. 2006), land ice exhibits a sawtooth,

whereas sea ice exhibits spikes. In Paillard and Parrenin (2004), ice volume resembles a sawtooth, while the ‘salty bottom waters formation efficiency’ (F) shows spikes. For the biased Van der Pol oscillator [introduced in Crucifix (2011) and investigated in detail in Saedeleer et al. (2013)], sawtooth cycles in the ice volume variable x occur when the variable y exhibits spikes. A strategy to discriminate between different models would consist of the following:

1. Identify proxy records corresponding to each of the variables in the different models. For the sawtooth variable, the relevant proxy record will generally be marine $\delta^{18}\text{O}$; the relevant proxy record for the spiking variable depends on the specific interpretation of the model.
2. Test the amplitude-periodicity relationship for the sawtooth variable in each of the different models. In our view, the marine $\delta^{18}\text{O}$ record clearly indicates that the amplitude and periodicity of the sawtooth are approximately linearly proportional to each other (see Fig. 8b). This relationship probably holds for every model in which the slope of the slowly increasing part of the sawtooth is held constant, for example Huybers (2007). However, one would rather expect a square-root dependence, if the slow part of the sawtooth were due to a random-walk process, as suggested by Wunsch (2003).
3. Collect proxy records corresponding to the spiking variable(s) that span across a time period when the periodicity/amplitude of the glacial cycles increased (Early Pleistocene, MPT, Mid-Brunhes). In our model context, the records of interest would be calcifier productivity and calcite accumulation. That said, any record that shows systematic deglacial spikes that increase in magnitude whenever the amplitude of the glacial cycles increases could correspond to the actual spiking variable(s) driving the glacial-interglacial transitions. However, it is crucial that there is a compelling reason (such as a model prediction) to interpret the observed spikes as corresponding with a driver of the transition, rather than a responsive feedback.

If the forcing acts on the alkalinity input, rather than on the calcifiers directly, then the spikes are essentially triggered by the alkalinity alone. In this case, the response has the same periodicity as the forcing, unless the forcing amplitude is very large ($\alpha \sim 0.7$) and the initial state is very far from equilibrium. Although we do not know whether $\alpha \sim 0.7$ is unreasonably high, we think that the actual forcing probably operates on the spiking variable, because the cycles with different periodicities appear most robust in that case. Moreover, there exists more direct observational evidence for large variations in calcite accumulation (Beaufort et al. 1997; Herbert 1997) than for strong variations in the alkalinity input.

We have performed further simulations to investigate the sensitivity of the model to its key parameters. It turns out that some specific features are impacted rather strongly by the choice of parameter values. For example, increasing the calcifier mortality M (while keeping the other parameters constant) leads to:

1. a smaller average calcifier population
2. a higher average alkalinity
3. a transition to chaotic behavior at a lower forcing amplitude

Nevertheless, the basic sawtooth-spike behavior of the model is robust: it does not depend on specific combinations of parameter values. Moreover, the two key relationships identified in Sect. 3 are independent of parameter values, since these relationships emerge as inherent characteristics of the sawtooth-spike cycles.

Under the 20-kyr forcing, we obtained cycles with the well-known 20-, 40-, and 100-kyr periodicities, but we also found 60- and 80-kyr cycles: periodicities that are generally not found when spectral analysis is applied to paleoclimate records (Muller and MacDonald 1997; Petit et al. 1999; Ridgwell et al. 1999). We nevertheless focused our analysis on the results obtained under a 20-kyr forcing, because we did not find a robust 100-kyr periodicity under a 40-kyr forcing (as 100 is not a multiple of 40). However, the $\delta^{18}\text{O}$ data (Lisiecki and Raymo 2005) appear to suggest a dominant ~ 40 -kyr forcing. In fact, the lengths of individual glacial cycles identified from the Lisiecki and Raymo (2005) stack cluster into 3 distinct groups around 40, 80, and 120 kyr (Fig. 8b). These multiples of 40 kyr correspond with the periodicities that we obtained under the 40-kyr forcing (Fig. 5b). Perhaps, the primary forcing of the glacial-interglacial transitions is obliquity rather than precession, as has been argued before (Huybers and Wunsch 2005; Huybers 2007; Daruka and Ditlevsen 2014). Under this hypothesis, the post-MPT cycles are in fact alternating between ~ 80 - and ~ 120 -kyr modes, giving a 100-kyr periodicity on average.

The modeled periodicity shifts go in both directions, from short to long and from long to short, whereas the observations (Fig. 1) indicate a structural increase of the glacial periodicity throughout the Pleistocene. A structural increase in the periodicity of sawtooth cycles can be achieved in the model, if there is some positive feedback that increases the amplitude of the cycles over time. Again, this is due to the geometry of sawtooth cycles: a larger amplitude corresponds to a longer periodicity. One positive feedback within the context of the calcifier-alkalinity model would be a higher net input of alkalinity into the open ocean during glacial times.

However, it is unclear whether there exist significant glacial-interglacial variations in the alkalinity input; it may actually have stayed approximately constant over glacial-interglacial cycles (Munhoven 2002; Foster and Vance 2006). On one hand, silicate weathering increases with temperature (Walker et al. 1981; White et al. 1999) which should lead to a lower alkalinity input into the oceans during glacial times. On the other hand, a larger continental shelf area is above sea level during glacial times which should lead to a higher input of alkalinity due to carbonate weathering (Gibbs and Kump 1994; Jones et al. 2002) and a lower alkalinity output due to fewer coral reefs (Berger 1982). In any case, the cycles are enhanced if it is assumed that the net alkalinity input increases during glacial times, whereas the assumption of a decreased alkalinity input during glacial times leads to more damping of the cycles.

5 Conclusion

A forced calcifier-alkalinity model exhibits shifts in the dominant periodicity, akin to the MPT. These shifts result from an interplay between the different elements of the system, but the spiking variable (calcifiers) plays a key role, as it provides the memory hypothesized by Huybers (2009). In our view, this is further evidence that a spiking variable in the climate system must be playing an active role in glacial dynamics. Nevertheless, we wish to emphasize that our model features one mechanism that, in the real world, complements a host of processes. Based on these various processes, very different explanations for glacial dynamics have been proposed. To distinguish between different explanations, we believe that it is crucial to formulate predictions that can be tested against observations. In this study, we have provided two such predictions:

1. The amplitude and the periodicity of the cycles are approximately linearly proportional to each other, due to the constant slope of the slowly increasing part (set by the alkalinity input). The benthic $\delta^{18}\text{O}$ proxy data (Fig. 8b) indeed show such a linear proportionality which provides a clear constraint on the dynamics underlying the slow part of the sawtooth between the rapid transitions.
2. The magnitude of the spikes increases with increasing periodicity and amplitude of the sawtooth. This prediction could be used to identify one or more currently hidden spiking variables driving the glacial-interglacial transitions. Essentially, the quest would be for any proxy record, concurrent with a dynamical model prediction, that exhibits deglacial spikes which increase

at times when the amplitude/periodicity of the glacial cycles increases. In the specific context of our calcifier-alkalinity mechanism, the records of interest would be calcifier productivity and calcite accumulation. We believe that such a falsifiable hypothesis should provide a strong motivation for the collection of further records.

Acknowledgments We would like to thank Adina Paytan, Michel Crucifix, and an anonymous reviewer for helpful comments and Alexis Yelton for suggesting the title of the article. Anne Willem Omta and Mick Follows are grateful for support from the National Science Foundation (NSF) under Grant OCE-1155295. The work of George van Voorn was part of the strategic research program Knowledge Base IV (KBIV) ‘sustainable spatial development of ecosystems, landscapes, seas and regions’ funded by the Netherlands Ministry of Economic Affairs. Ros Rickaby was supported through European Research Council (ERC) Grant SP2-GA-2008-200915. Furthermore, Mick Follows is grateful for support from the NSF under Grant OCE-1259388.

Appendix 1: Bifurcation analysis

The phenomena observed in the simulations are underpinned by bifurcations in the model. Specialized numerical software such as AUTO (Doedel and Oldeman 2009) exists to perform bifurcation analysis. As a start-up it requires an equilibrium or a periodic orbit. Using so-called test functions the software then monitors the steady state from which one starts and the stability properties of this steady state under parameter change. The software indicates bifurcations by type.

When the parameter k changes periodically as given in Eq. (3), the system is nonautonomous and equilibria do not exist: there are only periodic and chaotic dynamics. To be able to use AUTO, an autonomous system is formulated through the introduction of two additional equations:

$$\frac{dx}{dt} = x + \omega y - x(x^2 + y^2), \quad (6a)$$

$$\frac{dy}{dt} = y - \omega x - y(x^2 + y^2). \quad (6b)$$

These equations asymptotically converge to a sinusoidal oscillation:

$$x = \sin(\omega t), \quad y = \cos(\omega t), \quad (7a)$$

$$\dot{x} = \omega \cos(\omega t), \quad \dot{y} = -\omega \sin(\omega t), \quad (7b)$$

which can be verified by substitution of the second set of equations into the first set, and by using $\cos^2(v) + \sin^2(v) = 1$. Thus, the periodic forcing is introduced with $\omega = 2\pi/T$ and $\theta = 0$:

$$k = k_0(1 + \alpha y) \quad (8)$$

The forcing amplitude α is now effectively used as a bifurcation parameter, and the model is rewritten as a periodic orbit continuation in *AUTO*, starting at $\alpha = 0$. Although these equations are not identical to the ones used for the time series simulations, they have the same asymptotic solutions. Moreover, the periodic asymptotic solutions have the same stability properties, because the forcing oscillator system is stable and is independent of the response of the calcifier-alkalinity system. These are the relevant criteria, because *AUTO* is for the analysis of asymptotic behaviors. We compared asymptotic solutions from both implementations and they are indeed the same.

The period-1 orbit can be found directly with *AUTO*. However, the other orbits have to be found by using *MATLAB* for numerical simulations, which after sufficient simulation time give approximated periodic orbits. The approximated periodic orbits can be converted into starting files for *AUTO*, where *AUTO* is able to obtain precise periodic orbits with the use of Newton corrections. Each of these periodic orbits is now continued as a function of α up to and beyond period-doubling bifurcations. The double-periodic orbits can in turn be continued in α up to period doubling bifurcations, eventually leading to a chaotic attractor. Close to chaos, there are many different periodic orbits, each with its own domain of attraction.

Unlike limit cycles, chaotic attractors have no single global maxima or minima but continuously different local maxima or minima. Chaotic attractors are therefore depicted by plotting dots that represent the value of the desired state variable whenever its time derivative changes from positive to negative (for maxima, or vice versa for minima) in a simulation with a fixed bifurcation parameter value. The transient phase of such a simulation is discarded. To avoid cluttering, the simulation is terminated once the dot density is sufficient for visualization. The whole procedure is then repeated for a new simulation with a slightly different bifurcation parameter value, and so forth.

Appendix 2: Multi-box simulations

To investigate the behavior of the calcifier-alkalinity system in a more realistic setup, we perform simulations with a multi-box model [described in detail in Omta et al. (2013)], including explicit competition between two plankton functional groups and a treatment of the carbonate compensation feedback as proposed by Zeebe and Westbroek (2003). In Omta et al. (2013), cycles were obtained with the same 20-kyr periodicity as the forcing. As in the simulations with the simplest calcifier-alkalinity model, we now apply

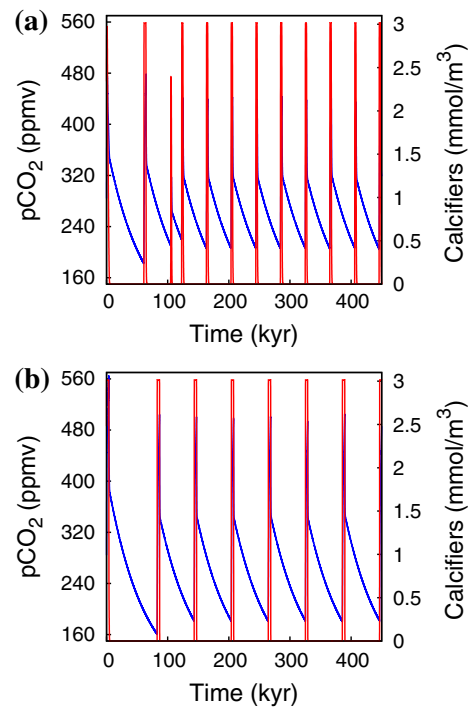


Fig. 9 Results from the multi-box model: atmospheric pCO₂ (blue) and calcifiers in the high-latitude box (red) as a function of time with $T = 20$ kyr and $\alpha = 0.002$ (a) and with $\alpha = 0.005$ (b)

a stronger periodic forcing to investigate whether longer cycles can arise; results are shown in Fig. 9. Overall, the simulations with a more complex and explicit model correspond with the basic result that under a sinusoidal forcing with a fixed period, the system response exhibits a variety of sawtooth cycles with different periodicities, each being a multiple of the forcing periodicity. As in the simulations with the more idealized model, a longer periodicity corresponds with a larger amplitude of the cycles (compare Fig. 9a, b). Moreover, a large periodicity and amplitude of the sawtooth correspond to a large magnitude of the spikes (primarily reflected in a longer duration of the spikes in Fig. 9b compared to Fig. 9a).

References

- Augustin L, Barbante C, Barnes PRF, Barnola JM, Bigler M, Castellano E, Cattani O, Chappellaz J, Dahl-Jensen D, Delmonte B, Dreyfus G, Durand G, Falourd S, Fischer H, Flückiger J, Hansson ME, Huybrechts P, Jugie G, Johnsen SJ, Jouzel J, Kaufmann P, Kipfstuhl J, Lambert F, Lipenkov VY, Littot GC, Longinelli A, Lorrain R, Maggi V, Masson-Delmotte V, Miller H, Mulvaney R, Oerlemans J, Oerter H, Orombelli G, Parrenin F, Peel DA, Petit JR, Raynaud D, Ritz C, Ruth U, Schwander J, Siegenthaler U, Souchez R, Stauffer B, Steffensen JP, Stenni B, Stocker TF, Tabacco IE, Udisti R, van de Wal RSW, van den Broeke M, Weiss J, Wilhelms F, Winther JG, Wolff EW, Zuchelli

- M (2004) Eight glacial cycles from an Antarctic ice core. *Nature* 429:623–628
- Beaufort L, Lancelot Y, Camberlin P, Cayre O, Vincent E, Bassinot F, Labeyrie L (1997) Insolation cycles as a major control of equatorial Indian Ocean primary production. *Science* 278:1451–1454
- Berger A, Li XS, Loutre MF (1999) Modelling Northern hemisphere ice volume over the last 3 Ma. *Quat Sci Rev* 18:1–11
- Berger A, Loutre MF (1991) Insolation values for the climate of the last 10 million years. *Quat Sci Rev* 10:297–317
- Berger AL (1978) Long-term variations of daily insolation and quaternary climatic changes. *J Atmos Sci* 35:2362–2367
- Berger WH (1982) Increase of carbon dioxide in the atmosphere during deglaciation: the coral reef hypothesis. *Naturwissenschaften* 69:87–88
- Bintanja R, van de Wal RSW (2008) North American ice-sheet dynamics and the onset of 100,000-year glacial cycles. *Nature* 45:869–872
- Clark PU, Pollard D (1998) Origin of the middle Pleistocene transition by ice sheet erosion of regolith. *Paleoceanography* 13:1–9
- Crowley TJ, Hyde WT (2008) Transient nature of late Pleistocene climate variability. *Nature* 456:226–230
- Crucifix M (2011) How can a glacial inception be predicted? *The Holocene* 21:831–842
- Crucifix M (2012) Oscillators and relaxation phenomena in Pleistocene climate theory. *Philos Trans R Soc A* 370:1140–1165
- Crucifix M (2013) Why could ice ages be unpredictable? *Clim Past* 9:2253–2267
- Daruka I, Ditlevsen PD (2014) Changing climate response: a conceptual model for glacial cycles and the Mid-Pleistocene Transition. *Clim Past Discuss* 10:1101–1127
- de Saedeleer B, Crucifix M, Wieczorek S (2013) Is the astronomical forcing a reliable and unique pacemaker for climate? A conceptual model study. *Clim Dyn* 40:273–294
- Denton GH, Anderson RF, Toggweiler JR, Edwards RL, Schaefer JM, Putnam AE (2010) The last glacial termination. *Science* 328:1652–1656
- Ditlevsen PD (2009) Bifurcation structure and noise-assisted transitions in the Pleistocene glacial cycles. *Paleoceanography* 24:PA3204
- Doedel EJ, Oldeman B (2009) AUTO07P: continuation and bifurcation software for ordinary differential equations. Concordia University, Montreal
- Elderfield H, Ferretti P, Greaves M, Crowhurst S, McCave IN, Hodell D, Piotrowski AM (2012) Evolution of ocean temperature and ice volume through the Mid-Pleistocene climate transition. *Science* 337:704–709
- Foster GL, Vance D (2006) Negligible glacial-interglacial variation in continental weathering rates. *Nature* 444:918–921
- Ghil M (1994) Cryothermodynamics: the chaotic dynamics of paleoclimate. *Physica D* 77:130–159
- Gibbs MT, Kump LR (1994) Global chemical erosion during the last glacial maximum and the present: sensitivity to changes in lithology and hydrology. *Paleoceanography* 9:529–543
- Gildor H, Tziperman E (2000) Sea ice as the glacial cycles' climate switch: role of seasonal and orbital forcing. *Paleoceanography* 15:605–615
- Gildor H, Tziperman E (2001) Physical mechanisms behind biogeochemical glacial-interglacial CO₂ variations. *Geophys Res Lett* 28:2421–2424
- Guckenheimer J, Holmes P (1985) Nonlinear oscillations, dynamical systems and bifurcations of vector fields. Springer, Berlin
- Herbert T (1997) A long marine history of carbon cycle modulation by orbital-climatic changes. *Proc Natl Acad Sci* 94:8362–8369
- Huybers PJ (2007) Glacial variability over the last two million years: an extended depth-derived age model, continuous obliquity pacing, and the Pleistocene progression. *Quat Sci Rev* 26:37–55
- Huybers PJ (2009) Pleistocene glacial variability as a chaotic response to obliquity forcing. *Clim Past* 5:481–488
- Huybers PJ, Curry WB (2006) Links between annual, Milankovitch and continuum temperature variability. *Nature* 441:329–332
- Huybers PJ, Wunsch C (2005) Obliquity pacing of the late Pleistocene glacial terminations. *Nature* 434:491–494
- Imbrie J, Berger A, Boyle EA, Clemens SC, Duffy A, Howard WR, Kukla G, Kutzbach J, Martinson DG, McIntyre A, Mix AC, Molino B, Morley JJ, Peterson LC, Pisias NG, Prell WL, Raymo ME, Shackleton NJ, Toggweiler JR (1993) On the structure and origin of major glaciation cycles: 2. The 100,000-year cycle. *Paleoceanography* 8:699–735
- Jaccard SL, Hayes CT, Martínez-García A, Hodell DA, Sigman DM, Haug GH (2013) Two modes of changes in Southern Ocean productivity over the past million years. *Science* 339:1419–1423
- Jones IW, Munhoven G, Tranter M, Huybrechts P, Sharp MJ (2002) Modelled glacial and non-glacial HCO₃⁻, Si and Ge fluxes since the LGM: little potential for impact on atmospheric CO₂ concentrations and a potential proxy of continental chemical erosion, the marine Ge/Si ratio. *Glob Planet Change* 33:139–153
- Kuznetsov YA, Muratori S, Rinaldi S (1992) Bifurcations and chaos in a periodic predator-prey model. *Int J Bifurcat Chaos* 2:117–128
- le Treut H, Ghil M (1983) Orbital forcing, climatic interactions, and glaciation cycles. *J Geophys Res* 88:5167–5190
- Lisiecki LE, Raymo ME (2005) A Pliocene–Pleistocene stack of 57 globally distributed benthic δ¹⁸O records. *Paleoceanography* 20:PA1003
- Liu Z, Herbert TD (2004) High-latitude influence on the eastern equatorial Pacific climate in the early Pleistocene epoch. *Nature* 427:720–723
- Lüthi D, le Floch M, Bereiter B, Blunier T, Barnola JM, Siegenthaler U, Raynaud D, Jouzel J, Fischer H, Kawamura K, Stocker TF (2008) High-resolution carbon dioxide concentration record 650,000–800,000 years before present. *Nature* 453:379–382
- Marlowe IT, Brassell SC, Eglinton G, Green JC (1990) Long-chain alkenones and alkyl alkenoates and the fossil coccolith record of marine sediments. *Chem Geol* 88:349–375
- Miles J (1988) Resonance and symmetry breaking for the pendulum. *Physica D* 31:252–268
- Milliman JD, Troy PJ, Balch WM, Adams AK, Li YH, Mackenzie FT (1999) Biologically mediated dissolution of calcium carbonate above the chemical lysocline? *Deep Sea Res I* 46:1653–1669
- Mitsui T, Aihara K (2014) Dynamics between order and chaos in conceptual models of glacial cycles. *Clim Dyn* 42:3087–3099
- Mudelsee M, Schulz M (1997) The Mid-Pleistocene climate transition: onset of 100-ka cycle lags ice-volume buildup by 280 ka. *Earth Planet Sci Lett* 151:117–123
- Muller RA, MacDonald GJ (1997) Spectrum of 100-kyr glacial cycle: orbital inclination, not eccentricity. *Proc Natl Acad Sci* 94:8329–8334
- Munhoven G (2002) Glacial-interglacial changes of continental weathering: estimates of the related CO₂ and HCO₃⁻ flux variations and their uncertainties. *Glob Planet Change* 33:155–176
- Omta AW, van Voorn GAK, Rickaby REM, Follows MJ (2013) On the potential role of marine calcifiers in glacial-interglacial dynamics. *Glob Biogeochem Cycles* 27:692–704
- Paillard D (1998) The timing of Pleistocene glaciations from a simple multiple-state climate model. *Nature* 391:378–381
- Paillard D, Parrenin F (2004) The Antarctic ice sheet and the triggering of deglaciations. *Earth Planet Sci Lett* 227:263–271
- Pelletier JD (1998) The power spectral density of atmospheric temperature from time scales of 10⁻² to 10⁶ yr. *Earth Planet Sci Lett* 158:157–164
- Petit JR, Jouzel J, Raynaud D, Barkov NI, Barnola JM, Basile I, Bender M, Chappellaz J, Davis M, Delaygue G, Delmotte M, Kotlyakov VM, Legrand M, Lipenkov VY, Lorius C, Pépin L,

- Ritz C, Saltzman E, Stievenard M (1999) Climate and atmospheric history of the past 420,000 years from the Vostok ice core, Antarctica. *Nature* 399:429–436
- Raymo ME, Lisiecki LE, Nisancioglu KH (2006) Plio-Pleistocene ice volume, Antarctic climate and the global $\delta^{18}\text{O}$ record. *Science* 313:492–495
- Rial JA, Oh J, Reischmann E (2013) Synchronization of the climate system to eccentricity forcing and the 100,000-year problem. *Nat Geosci* 6:289–293
- Ridgwell A, Watson AJ, Raymo ME (1999) Is the spectral signature of the 100 kyr glacial cycle consistent with a Milankovitch origin? *Paleoceanography* 14:437–440
- Rinaldi S, Muratori S (1993) Conditioned chaos in seasonally perturbed predator-prey models. *Ecol Model* 69:79–97
- Saltzman B, Maasch KA (1991) A first-order global model of late Cenozoic climatic change. II. Further analysis based on a simplification of the CO_2 dynamics. *Clim Dyn* 5:201–210
- Schefuss E, Jansen JHF, Sinninghe-Damsté JS (2005) Tropical environmental changes at the mid-Pleistocene transition: insights from lipid biomarkers. In: Head MJ, Gibbard PL (eds) Early-middle Pleistocene transitions: the land-ocean evidence. The Geological Society, Bath, pp 35–63
- Schoepfer SD, Shen J, Wei H, Tyson RV, Ingall E, Algeo TJ (2015) Total organic carbon, organic phosphorus, and biogenic barium fluxes as proxies for paleomarine productivity. *Earth Sci Rev* 146:49–78
- Schulz KG, Zeebe RE (2006) Pleistocene glacial terminations triggered by synchronous changes in Southern and Northern insolation: the insolation canon hypothesis. *Earth Planet Sci Lett* 249:326–336
- Sexton PF, Barker S (2012) Onset of ‘Pacific-style’ deep-sea sedimentary carbonate cycles at the mid-Pleistocene transition. *Earth Planet Sci Lett* 321/322:81–94
- Tian J, Pak DK, Wang P, Lea D, Cheng X, Zhao Q (2006) Late Pliocene monsoon linkage in the tropical South China Sea. *Earth Planet Sci Lett* 252:72–81
- Tziperman E, Gildor H (2003) On the mid-Pleistocene transition to 100-kyr glacial cycles and the asymmetry between glaciation and deglaciation times. *Paleoceanography* 18:1001
- Tziperman E, Raymo ME, Huybers PJ, Wunsch C (2006) Consequences of pacing the Pleistocene 100 kyr ice ages by nonlinear phase locking to Milankovitch forcing. *Paleoceanography* 21:PA4206
- Walker JGC, Hays PB, Kasting JF (1981) A negative feedback mechanism for the long-term stabilization of Earth’s surface temperature. *J Geophys Res* 86:9776–9782
- White AF, Blum AE, Bullen TD, Vivit DV, Schultz M, Fitzpatrick J (1999) The effect of temperature on experimental and natural chemical weathering rates of granitoid rocks. *Geochim Cosmochim Acta* 63:3277–3291
- Wiggins S (1990) Introduction to applied nonlinear dynamical systems and chaos. Springer, New York
- Wunsch C (2003) The spectral description of climate change including the 100 ky energy. *Clim Dyn* 20:353–363
- Zeebe RE, Westbroek P (2003) A simple model for the CaCO_3 saturation state of the ocean: the ‘Strangelove’, the ‘Neritan’, and the ‘Cretan’ Ocean. *Geochem Geophys Geosyst* 4:1104